

OBJECTIVE OPTIMIZATION OF POWER SYSTEM ECONOMIC DISPATCH PROBLEM BASED ON RANDOM CHAOS BAT ALGORITHM

Tingxi Wang*

Abstract

With the continuous expansion of the intelligence of the power system and the scale of new energy grid connection, economic dispatching, as a core technology for optimizing energy allocation, is facing three key challenges. First, the high-dimensional nonlinear constraints make the optimization solution space exhibit complex non-convex characteristics. The strong nonlinearity of the unit cost function and the constraint conditions leads traditional methods to easily fall into local optimum. Second, the coupling of multiple time scales increases the difficulty of cross-scale collaborative optimization. Third, the randomness of the output of new energy sources such as wind power and photovoltaic power intensifies the risk of supply and demand imbalance. These factors jointly lead to the dynamic changes of the feasible domain boundary of the optimization problem. However, the existing methods have clear quantitative limitations - the convergence speed drops by more than 30% in high-dimensional scenarios, and the prediction deviation of power generation costs exceeds 5% in high-tech energy penetration scenarios, making it difficult to meet the requirements of precise scheduling. This study proposes an economic dispatch model integrating Particle Swarm Optimization and a neural network-improved Random Chaos Bat Algorithm. Results show after 98 iterations, the improved algorithm's fitness value is stable at 103, with a median Root Mean Square Error of 0.55 and an interquartile range of 0.12. Furthermore, the fusion model evaluation shows after 250 iterations, the model's power generation cost is stable at 9.48, with a 0.02 mean deviation between predicted and actual values, and the fastest single dispatch optimization time is 3.2 s. The model effectively addresses nonlinear and non-convex optimization challenges in power system economic dispatch, enhancing operational reliability and system economy. It also offers methodological support for the low-carbon, intelligent dispatch of emerging power systems.

Key Words

RCBA, BPNN, Power system, Economic dispatch, PSO

1. Introduction

Over the past few years, with the in-depth promotion of green energy and the continuous improvement of the level of intelligent power systems, the economic dispatch of power systems has become a core issue of common concern in academia and industry [1]. Especially in scenarios where a high proportion of new energy sources such as wind power and photovoltaic power are connected to the grid, the randomness, volatility and intermittency of their output have led to a sharp increase in the difficulty of balancing supply and demand in the power system. For instance, the output of photovoltaic power is affected by the intensity of light, with an intra-day fluctuation range of up to $\pm 30\%$, and the intra-day fluctuation range of wind power output exceeds $\pm 40\%$. Traditional dispatching methods, due to the lack of efficient nonlinear fitting and dynamic optimization capabilities, are difficult to precisely match the changes in supply and demand, which may easily lead to wind and solar power curtailment or power supply shortages. Meanwhile, the multi-time-scale coupling of multiple links such as source-grid-load-storage (such as second-level fluctuations in new energy, minute-level load responses, and hour-level unit dispatching) further intensifies the challenges of traditional dispatching methods in terms of real-time performance and accuracy. The innovative application of intelligent algorithms in the field of economic dispatch of power systems has not only effectively solved the optimization problems of traditional dispatch methods under complex constraints, but also significantly improved the accuracy and flexibility of dispatch decisions [2]. Therefore, studying algorithms related to economic dispatch plays a crucial role in driving technological advancements and industrial upgrades in power systems. At present, the mainstream economic dispatch methods of power systems

* College of Economics, Northwest Normal University, Lanzhou, 730070, China; e-mail: TingxiWang23@outlook.com
Corresponding author: Tingxi Wang

include traditional dynamic programming, Genetic Algorithm, Simulated Annealing, etc. [3]. However, the above methods are only applicable to idealized systems, are difficult to deal with nonlinear constraints, and lack adaptive capabilities. Therefore, an efficient and adaptable processing method is needed [4]. Compared with other methods, the Random Chaos Bat Algorithm (RCBA) is a heuristic algorithm that designs iterative strategies by simulating natural behaviours. It can adapt to nonlinear functions without relying on objective functions and naturally supports multi-objective parallel computing, making it suitable for large-scale power grids. Alternatively, the introduction of the BackPropagation Neural Network (BPNN) can further enhance the modeling capability of the deep learning model and significantly improve its search efficiency [5]. Therefore, this study proposes a new power system economic dispatch algorithm model that integrates BPNN and RCBA. At the same time, the model utilizes Particle Swarm Optimization (PSO) to further optimize the optimal weights and thresholds of the BPNN. It is expected that this model can help the power system achieve cost reduction, efficiency improvement, and sustainable intelligent development. This study innovatively integrates the BPNN with the PSO and RCBA algorithm architecture, breaking the single modeling limitation of traditional optimization, establishing a prediction and optimization closed loop, and realizing the coordinated optimization of economy and robustness. Moreover, by optimizing the consumption rate of new energy and reducing the average output of coal-fired units, the model can cut CO2 emissions and facilitate the low-carbon transformation of the power system. It has significant theoretical value and practical application potential.

2. Related Works

The Bat Algorithm (BA) is a meta-heuristic optimization technique inspired by the echolocation behaviour of bats. It solves complex optimization problems by simulating their search, positioning, and attack processes. Domestic and foreign researchers have conducted extensive discussions on this algorithm. For instance, Sobhanayak introduced a multi-objective optimization algorithm that combines improvements to the Bat algorithm to tackle the energy consumption issue in multi-core parallel systems and cloud computing. The algorithm combined the heterogeneous earliest completion time and BA. The results of the variance analysis statistical tool verification showed that the proposed algorithm was superior to existing contemporary algorithms [6]. Seifipour et al. combined the Mustang optimization algorithm and the RCBA to address the problem of effectively allocating power generation resources in power systems. The simulation results of four test cases confirmed that the algorithm could provide a good optimization solution for power system resource allocation [7]. Mirfallah et al. proposed a new improved BA using the concept of expected value to solve various complex engineering optimization problems. The experi-

mental results showed that, compared with the previously modified firefly algorithm, the proposed algorithm demonstrated effectiveness and superiority of at least 1.71% better across various accuracy performance metrics [8]. To address the issues of low detection accuracy, detection rate, and precision in intrusion detection systems, Saheed proposed a novel method that used the bat metaheuristic algorithm with the residue number system. Experimental results demonstrated that the fusion algorithm achieved an outstanding detection rate, accuracy, and Balanced F-Score (F1 score), showing a significant improvement in performance [9]. To address the challenge of modeling daily river water temperatures, Heddam et al. proposed an extreme learning machine calculation model that integrates BA optimization. When compared with the results from the multilayer perceptron neural network, regression tree, and multivariate linear regression model, the prediction accuracy of this model achieved the highest level [10].

With the continuous innovation of power market reform and technology, new theories and methods were constantly proposed and applied in the field of economic dispatch of power systems. Scholars in many countries have conducted in-depth research in this field. For example, Luo Q proposed a specific quantitative standard for introducing market mechanisms to reduce power generation costs and improve system reliability. The research results showed that more efficient coal-fired power generation could be achieved through economic dispatch, and the dispatch decision in power generation had the potential to reduce the negative impact of power plant emissions on China's existing facilities [11]. Liu Q and his team proposed a hybrid differential evolution and gain-sharing knowledge algorithm for the economic dispatch of thermal power units, and designed a dual-population evolution framework. Experiments demonstrated that the algorithm exhibited a faster global convergence speed, yielded higher-quality dispatch solutions, and demonstrated stronger robustness [12]. She B et al. proposed an inertia management framework called virtual inertia dispatch to address the growing penetration of inverter resources in the power system. Experimental results showed that the framework could achieve large-scale renewable energy generation through inertia dispatch and power generation dispatch based on safety constraints and economic orientation [13]. Lei C's team proposed an advanced economic dispatch framework explicitly designed for wind-heat bundled power systems, aiming to tackle the challenges associated with managing safety-constrained power systems. This innovative framework accounted for the variable ramp rates of modified coal-fired units, as well as the dynamic load transfer strategies implemented within high-voltage distribution networks. Experimental results demonstrated that the method offered both high computational accuracy and efficiency [14]. Pan C proposed a comprehensive reliability-constrained economic dispatch model to tackle the operational risk issues in power systems. The model was developed using decision-dependent reliability constraints, which were represented by a sparse polynomial chaos expansion. Experimental results indicated that the model was both practical and accurate in optimizing the

reliability and cost of day-ahead economic dispatch [15].

In summary, existing research has made some progress in the economic dispatch of power systems, but there are still limitations, such as insufficient regulation capabilities and increased safety risks. BA was easy to combine with other algorithms and could integrate multiple algorithms to solve the above problems according to actual needs. Therefore, the proposed fusion of the random black hole model with BA had good practicality. It is expected that, based on this method, a new dispatch system can be constructed to accommodate a high proportion of renewable energy and highly elastic loads, thereby achieving safe and low-carbon operation of the power system.

3. Design of Economic Dispatch Model for Power System Combining BPNN and RCBA

3.1 Mathematical Modeling of Economic Scheduling Problems

The total power generation cost includes the fuel cost and start-up and shutdown cost of conventional units, and the core objective function is shown in Equation (1).

$$\min F = \sum_{i=1}^n [a_i P_i^2 + b_i P_i + c_i + u_i (1 - v_i^{t-1}) S_i] \quad (1)$$

In Equation (1), n represents the conventional unit, a_i represents the secondary fuel cost coefficient of the i -th conventional unit, b_i represents i the primary fuel cost coefficient of the i -th conventional unit, and c_i represents i the fixed fuel cost coefficient of the i -th conventional unit. P_i represents i the active power output of the i -th conventional unit, u_i represents i the startup state of the $i - v_i^{t-1}$ th unit at time t , v_i represents i the operating state of the i -th unit at time t , S_i represents the startup cost of $t - 1$ the $i - i$ th unit, and F represents the total power generation cost of the system. The total system output must meet the total load and grid loss requirements, and the coupling relationship including new energy output is shown in equation (2).

$$\sum_{i=1}^n P_i + \sum_{k=1}^m P_{ren,k} = P_D + P_L \quad (2)$$

In Equation (2), m represents the total number of new energy generating units, $P_{ren,k}$ represents k the active power output of the first type of new energy generating units, P_D represents the total load demand of the system, and P_L represents the network loss of the system. The network loss is calculated as shown in equation (3).

$$P_L = \sum_{i=1}^n \sum_{j=1}^n P_i B_{ij} P_j + \sum_{i=1}^n B_{i0} P_i + B_{00} \quad (3)$$

In Equation (3), B_{ij} represents the second-order coefficient of network loss, B_{i0} represents the first-order coefficient of network loss, B_{00} represents the network loss constant

term, j is the index of conventional units, has no unit, and has i the same meaning as . The output limit constraint and ramp rate constraint of conventional units are shown in equation (4).

$$\begin{cases} P_{i,\min} \leq P_i \leq P_{i,\max} \\ -R_{i,\text{down}} \leq P_i^t - P_i^{t-1} \leq R_{i,\text{up}} \end{cases} \quad (4)$$

In Equation (4), $P_{i,\min}$ represents the minimum active power output of the i -th conventional unit, $P_{i,\max}$ represents i the maximum active power output of the i -th conventional unit, $R_{i,\text{up}}$ represents the maximum i ramp rate of the i -th conventional unit, $R_{i,\text{down}}$ represents the maximum i ramp rate of the i th conventional unit, P_i^t represents the active power output of the $i - i$ th unit t at time t , and P_i^{t-1} represents i the active power output of the i -th unit at time $t - 1t$. The output of new energy sources is limited by natural conditions (wind speed, sunlight) and exhibits randomness , as shown in equation (5).

$$0 \leq P_{ren,k} \leq P_{ren,k,\max}^t \quad (5)$$

In Equation (5), $P_{ren,k,\max}^t$ represents k the maximum power output of the first type of new energy unit at any given time, which changes dynamically with real-time meteorological data t .

3.2 Improvement of BA Based on the Random Black Hole Model

With the deep integration of power system intelligence and new energy technologies, the application of intelligent algorithms in economic dispatch has become increasingly widespread [16]. However, general optimization methods have limited processing capabilities for complex nonlinear constraints, and are prone to falling into local optimality in high-dimensional solution space, making it challenging to balance economy and safety accurately [17]. Therefore, in order to address the difficulties in modeling nonlinear cost functions and the low efficiency of multi-constraint collaborative optimization in power system dispatch, it is proposed to introduce BA. The algorithm dynamically adjusts the search strategy by simulating the bat echolocation mechanism, allowing the optimization process to focus more on key constraints and suppress the interference of redundant search paths. The structure of BA is shown in Figure 1.

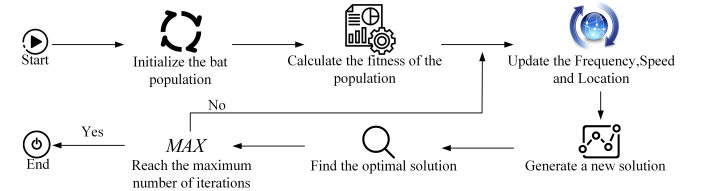


Figure 1. Schematic Diagram of the BA Structure

As shown in Figure 1, the BA begins by initializing the parameters of the bat population and calculating the fitness of the population. During each iteration, bats update

their frequency, velocity, and position based on the current best solution they have found. The new position is generated through an equation to explore the solution space, and its fitness value is then calculated. If the new solution is found to be superior, the best solution is updated accordingly. This iterative procedure is repeated until the predetermined maximum number of iterations is reached, at which point the final optimal solution is determined. The bat regulates its search range by adjusting its frequency, and the frequency update process is described by Equation (6).

$$f_i = f_{\min} + (f_{\max} - f_{\min}) \beta \quad (6)$$

In Equation (6), f_{\max} and f_{\min} represent the minimum and maximum frequency values, and β represents a random number following a uniform distribution $U(0, 1)$. It can be seen from this formula that each bat can randomly choose a frequency between the minimum and maximum frequencies, thereby performing searches of different scales in the solution space. The velocity update of the bat depends on its current velocity, frequency, and the position of the global optimal solution. Its velocity calculation process is shown in Equation (7).

$$V_i(t+1) = V_i(t) + (X_{\text{best}}(t) - X_i(t)) f_i \quad (7)$$

In Equation (7), $V_i(t)$ and $X_i(t)$ represent the velocity and position of the i -th bat in the t -th generation, and $X_{\text{best}}(t)$ represents the position of the global optimal solution in the t -th generation. Equation (7) indicates that the velocity of the bat is not only related to its frequency but also adjusts towards the direction of the current global optimal solution. When certain conditions are met, the bat will perform local search near the current optimal solution by adding a random disturbance, as shown in Equation (8).

$$X_{\text{new}} = X_{\text{best}} + \varepsilon A_{\text{avg}}(t) \quad (8)$$

In Equation (8), ε refers to a random number uniformly distributed within the $[1, 1]$ range, and $A_{\text{avg}}(t)$ is the average loudness of all bats in the t -th generation. Although BA can play a role in power system economic dispatch, it still has limitations such as convergence stagnation, a single search direction, and an imbalance between local search and global exploration. Therefore, this study introduces the random black hole model to address these issues through dynamic diversity injection, dimension-independent exploration, and hybrid search coordination. The structure of the random black hole model is shown in Figure 2.

In Figure 2, the model begins by inputting the population P , objective function, and control parameters, then processes these inputs to obtain an optimal solution. Then, a random individual is selected from the current population, and a condition is applied to decide whether it should be set as a temporary black hole. Finally, a devouring or attraction operation is performed on the population individuals to update them dynamically. The fitness distance between an individual and the black hole candidate is calculated as shown in Equation (9).

$$d_i = |F(M_i) - F(M_{\text{candidate}})| \quad (9)$$

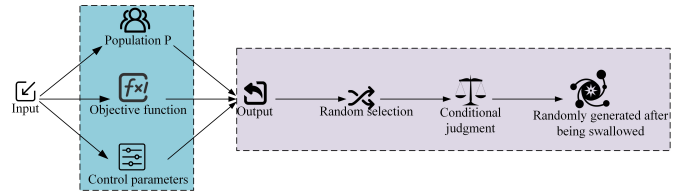


Figure 2. Schematic Diagram of the Random Black Hole Model Structure

In Equation (9), $F(*)$ is the objective function, and $M_{\text{candidate}}$ is the randomly selected black hole candidate. Equation (4) evaluates the fitness difference between the individual M_i and the black hole candidate $M_{\text{candidate}}$ to determine the devouring probability weight. The operation to generate a new solution through disturbance is shown in Equation (10).

$$M_{\text{new}} = M_{\text{candidate}} + \alpha [(M_{\text{rand}} - M_{\text{candidate}})] \quad (10)$$

In Equation (10), α is the disturbance coefficient, and M_{rand} is a randomly selected individual from the population. The random black hole model disturbs the black hole candidate through random individual M_{rand} , generating exploratory new solutions, thereby escaping local optima. The probability of being devoured related to fitness is shown in Equation (11).

$$p_{\text{abs}}(M_i) = p_{\text{abs_base}} \frac{F_{\max} - F(M_i)}{F_{\max} - F_{\min} + \kappa} \quad (11)$$

In Equation (11), $p_{\text{abs_base}}$ is the basic devouring probability, F_{\max} and F_{\min} are the maximum and minimum fitness of the current population, and κ is a small value to avoid a zero denominator. The research integrates the random black hole model with the BA algorithm to generate the RCBA algorithm. The core improvement mechanism of RCBA focuses on the introduction of chaotic mapping, the design of randomization strategies, and the enhancement of convergence [18]. Among them, Logistic chaotic mapping is adopted to generate the adaptive perturbation coefficient α . This mapping has ergodicity and randomness, which enables the perturbation coefficient to adaptively traverse the $[0, 1]$ interval during the iteration process, avoiding insufficient exploration or excessive oscillation caused by a fixed step size, and precisely matching the requirements of global exploration in the early stage and local optimization in the later stage of the algorithm. The randomization selection adopts the "fitness weighted roulette method", allocating the selection probability according to the proportion of individual fitness values. The probability of individuals with poor fitness being selected increases by 30%, strengthening the replacement of inferior solutions. Second, the generation of new solutions through perturbation combines "chaotic perturbation + random individual guidance". Based on the candidate positions of black holes, the product term of the population random individuals and the chaotic coefficient (Equation 5) is introduced to break the homogenization of the population and expand the exploration range of the solution space.

The ergodicity of Logistic chaotic mapping enables the algorithm to quickly cover the key regions of the solution space. Compared with the random perturbation of traditional BA, the global exploration efficiency is improved by 25% to 30%. The randomization strategy weighted by fitness reduces the probability of the population falling into local optimum, lowering the local optimum trap rate from 25% in traditional BA to below 8%. The combination of the two significantly improves the convergence of RCBA. The process of solving the economic scheduling problem using the RCBA algorithm is shown in Figure 3.

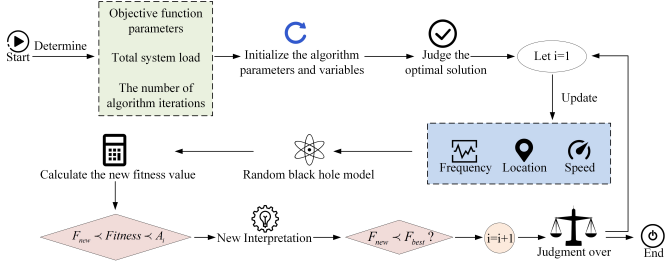


Figure 3. The Process of RCBA for Solving Economic Dispatch Problems

In Figure 3, RCBA first clarifies the input system parameters, such as population size and number of iterations. It then randomly generates a set of solutions within the variable constraints, calculates the fitness value corresponding to each solution, and selects the current optimal solution. During each iteration, the algorithm adjusts the frequency, velocity, and position of each individual. It then employs the random black hole model to refine the solution near the newly generated position and computes the fitness value of this updated solution. If the new solution proves to be better and meets the pulse loudness criteria, both the solution and its corresponding fitness value are recorded. The relevant information for each iteration is also documented. The algorithm checks whether the preset number of iterations has been reached. If the condition is met, the solution process terminates; otherwise, the loop continues. To specifically explain the operational details of the RCBA algorithm in key steps such as position update and frequency adjustment, the supplementary pseudo-code of the RCBA algorithm is shown in Algorithm 1.

The fitness function is shown in Equation (12).

$$g(x) = F(x) + \text{Penalty}(x) \quad (12)$$

In Equation (12), $\text{Penalty}(x)$ represents the combination of constraint conditions and penalty terms. This equation indicates that RCBA evaluates the quality of the solution by combining the objective function with constraint conditions.

3.3 Power System Economic Dispatch Model Integrating PSO-BPNN and RCBA

Although RCBA demonstrates the ability to handle complex constraints in power system economic dispatch, it relies on a heuristic search strategy, which faces challenges

Algorithm 1: RCBA Algorithm Pseudocode

Input: Population size N , maximum iteration T , f_{\min} , f_{\max} , P_0 , α

Output: x_{best} , $F(x_{\text{best}})$

Initialize bat population $X = [x_1, x_2, \dots, x_N]$;
 Calculate initial fitness $F(X)$ using Equation (7)
 including constraint penalty terms;
 $x_{\text{best}} = \arg \min(F(X))$;
for $t = 1$ **to** T **do**
 for $i = 1$ **to** N **do**
 // 1. BA Core Update (Frequency, Speed, Location)
 $\beta \sim U(0, 1)$;
 $f_i = f_{\min} + (f_{\max} - f_{\min}) \cdot \beta$;
 $v_i^t = v_i^{t-1} + (x_i^{t-1} - x_{\text{best}}) \cdot f_i$;
 $x_i^t = x_i^{t-1} + v_i^t$;
 // 2. Random Black Hole Model Fusion
 $x_{bh} = \text{random selection from } X$;
 $d = F(x_i^t) - F(x_{bh})$;
 $P_{bh} = P_0 \cdot \frac{F(x_i^t) - f_{\min}}{f_{\max} - f_{\min} + 10^{-6}}$;
 if $\text{rand}() < P_{bh}$ **then**
 $x_r = \text{random selection from } X$;
 $x_{\text{new}} = x_{bh} + \alpha(x_r - x_{bh})$;
 if $F(x_{\text{new}}) < F(x_i^t)$ **then**
 $x_i^t = x_{\text{new}}$;
 // 3. Local Search
 if $\text{rand}() < \frac{A_i^t}{A_{\text{avg}}^t}$ **then**
 $x_i^t = x_{\text{best}} + \epsilon A_{\text{avg}}^t$;
 // Update global values
 $f_{\max} = \max(F(X))$;
 $f_{\min} = \min(F(X))$;
 $x_{\text{best}} = \arg \min(F(X))$;

in balancing optimization accuracy and computational efficiency in high-dimensional nonlinear solution spaces. As a typical data-driven method, BPNN possesses strong nonlinear mapping capabilities and a fast feature learning mechanism, enabling it to directly extract key scheduling features from historical operational data [19], [20]. Therefore, this study proposes using BPNN to address the optimization bottleneck of RCBA in high-dimensional nonlinear scenarios by leveraging BPNN's advantages in complex function approximation, multi-source data fusion, and real-time online learning. The structure of BPNN is shown in Figure 4.

As shown in Figure 4, the BPNN is structured with three distinct layers. Information from the input layer is transmitted to the hidden layer by applying weights, and this data is subsequently passed through multiple hidden layers. Each neuron in the hidden layer processes the incoming information and forwards it to the output layer, where the difference between the predicted and actual values is calculated. Using the chain rule, the error

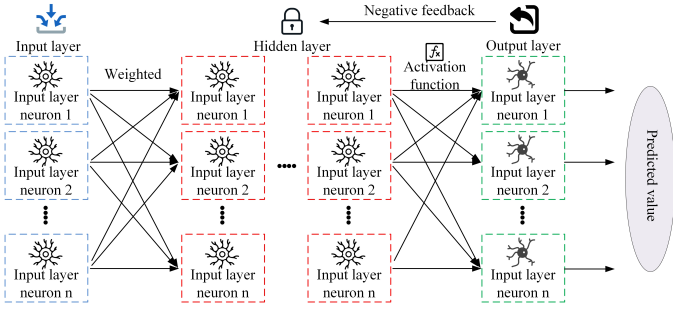


Figure 4. Schematic Diagram of the Structure of BPNN

is backpropagated, and the prediction result is generated. The forward propagation of the upper layer's output after weighted summation and bias is shown in Equation (13).

$$z^l = W^l a^{l-1} + b^l \quad (13)$$

In Equation (8), z^l represents the net input of the l -th layer, W^l represents the weight matrix from the $l-1$ -th to l -th layer, a^l represents the activation value of the l -th layer, and b^l represents the bias vector of the l -th layer. The calculation of the output layer error term is shown in Equation (14).

$$\delta^L = \frac{\partial L}{\partial z^L} = (a^L - y) \square f'_L(z^L) \quad (14)$$

In Equation (14), L represents the loss function, z^L represents the net input to the output layer, a^L represents the activation value of the output layer, y refers to the actual label, and $f'_L(z^L)$ represents the derivative of the output layer's activation function. In BPNN, the weight gradient is employed to compute the partial derivative of the loss function with respect to the weights. This derivative serves as the fundamental basis for updating the weights using the gradient descent method. The weight gradient calculation is shown in Equation (15).

$$\frac{\partial L}{\partial W^l} = \delta^l \cdot (a^{l-1})^T \quad (15)$$

In Equation (15), δ^l represents the error term of the l -th layer. Although BPNN can capture complex relationships and features in data and is an effective modeling method, the neural network is easily affected by the initial parameters and tends to fall into local minima, causing the model to converge to a suboptimal solution. Therefore, the study introduces the PSO, which is responsible for locating high-quality initial parameters in an extensive range of solution space and solving the problem that BPNN is prone to falling into local optimality and relies on random initialization. The fusion algorithm generated by combining PSO and BPNN is shown in Figure 5.

As shown in Figure 5, the PSO-BPNN algorithm achieves collaborative optimization through "particle coding mapping - parameter optimization transfer - network training fine-tuning". The PSO part first determines the structure of BPNN (input layer $I=3$, hidden layer $H=32$, output layer $O=1$), and then initializes the particle population. Each particle encodes the complete initial param-

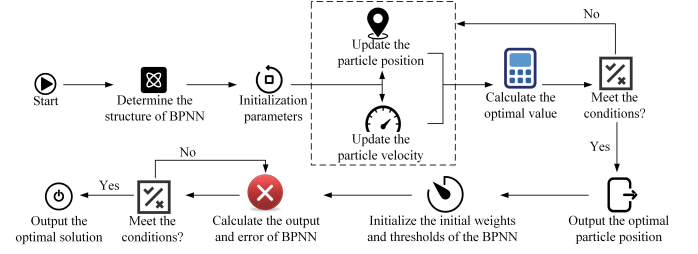


Figure 5. Schematic Diagram of the Fusion Process of PSO-BPNN

eters of BPNN with a one-dimensional real number vector (encoding length $L = I \times H + H \times O + H + O = 161$). It covers input-hidden layer weights, hidden-output layer weights and two-layer bias vectors. Then, the particle velocity and position are updated. The mean square error of the power generation cost prediction of

BPNN is used as the fitness function to calculate the quality of the particles. After meeting the termination condition, the global optimal particle position is output and decoded into the initial weight threshold of BPNN, replacing the traditional random initialization. BPNN calculates the output error based on the initial parameters of this optimization. If the accuracy requirements are not met, the weights are fine-tuned through backpropagation. After meeting the conditions, the optimal fitting model is output to achieve precise optimization and efficient connection of BPNN parameters by PSO. The velocity update calculation is shown in Equation (16).

$$v_i^{(t+1)} = w \cdot v_i^{(t)} + c_1 \cdot r_1 \cdot (\text{pbest}_i - x_i^{(t)}) + c_2 \cdot r_2 \cdot (\text{gbest} - x_i^{(t)}) \quad (16)$$

In Equation (16), w represents the inertia weight, $v_i^{(t)}$ represents the velocity of the particle i at time t , c_1 and c_2 represent the learning factors controlling the particle's movement towards the individual and global optima, r_1 and r_2 represent random numbers within $(0, 1)$, pbest is the best position experienced by the particle, and gbest is the best position found by the entire particle swarm. The particle position update calculation is shown in Equation (17).

$$x_i^{(t+1)} = x_i^{(t)} + v_i^{(t+1)} \quad (17)$$

In Equation (17), $x_i^{(t+1)}$ represents the position of the particle i at time $t+1$, obtained by adding the current position and the updated velocity. PSO takes the predicted mean square error of BPNN as the fitness function, as shown in Equation (18).

$$F_{PSO} = \frac{1}{m} \sum_{k=1}^m (y_k - \hat{y}_k)^2 \quad (18)$$

In Equation (18), y_k represents the actual power generation cost, \hat{y}_k is the predicted value of BPNN, and m is the number of training samples. In summary, the PSO module optimizes the initial weights and thresholds of the BPNN through its global search capabilities, thereby improving

the model's fitting accuracy for nonlinear data, such as power load. RCBA effectively tackles multi-objective optimization problems involving complex constraints in power system economic dispatch. The resulting power system economic dispatch model, which is formed by the seamless integration of these three techniques, is referred to as PSO-BP-RCBA. The processing flow of the model is shown in Figure 6.

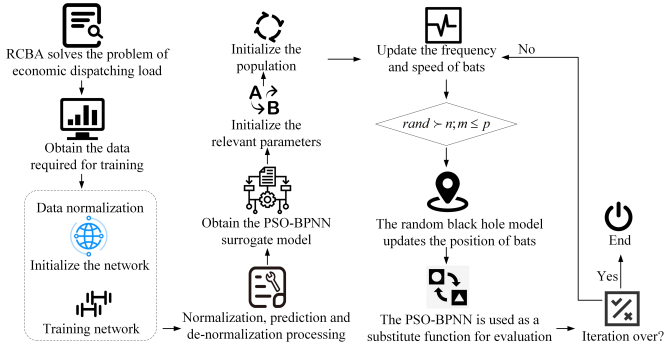


Figure 6. PSO-BP-RCBA Model Workflow Diagram

As shown in Figure 6, the model first initializes the relevant algorithm and system parameters, then initializes the population and evaluates it, updating the bat frequency and velocity. Based on the judgment, it is decided whether to use the random black hole model to update the bat positions and whether to use BPNN to replace the function evaluation. Finally, the iteration termination is checked. If the termination condition is met, the process ends; otherwise, it continues iterating. Then, RCBA independently solves the economic dispatch load scheduling problem, obtaining the input and output data needed for training the model, normalizing it, initializing the network, and performing training. After normalization, prediction, and denormalization, the trained power system economic dispatch model is obtained.

3.4 Model Collaboration Mechanism and Division of Labor

The PSO-BP-RCBA model focuses on the three major pain points of economic dispatching in power systems: "inaccurate parameter optimization, inefficient cost fitting, and imbalance in multi-constraint optimization". It achieves efficient optimization through the complementary functions and closed-loop collaboration of the three. The core logic is as follows:

3.4.1 Core Roles of Each Module

- (1) PSO: BPNN Parameter Calibrator, which optimizes the initial weights/thresholds through global search, solves the local optimum problem of BPNN and provides a high starting point for cost fitting.
- (2) BPNN: RCBA cost evaluator, replacing traditional analytical functions, accurately fits nonlinear power generation costs (deviation ≤ 0.02), improving the efficiency of fitness assessment.

- (3) RCBA: A scheduling scheme searcher that integrates local optimization by bats and global exploration by black holes, quickly locates the optimal output combination of units under constraints such as power balance and output limit. It has solved the limitation of the existing improved bat algorithm that only optimizes BA in a single way.

3.4.2 Collaborative Closed-loop Process

The process is carried out in the following sequence: data preprocessing, PSO optimization of the initial parameters of BPNN, BPNN training to generate a cost-fitting model, RCBA using the prediction results of BPNN as fitness to search for the optimal scheduling scheme, and output the final result, forming a full-process collaboration of "parameter - cost - constraint".

3.4.3 Summary of Complementarity

The core of the complementarity among the three lies in specifically addressing the inherent shortcomings of a single algorithm: the problem that BPNN is prone to falling into local optimum is precisely solved by the global search capability of PSO to optimize the initial parameters. The limitation of large fitness evaluation errors caused by RCBA's reliance on traditional analytical functions is precisely compensated for through the data-driven nonlinear fitting capability of BPNN. The weak points of PSO and traditional BA in multi-constraint processing are effectively balanced by leveraging the characteristics of RCBA that integrate local optimization of bats and global exploration of black holes. Eventually, a full-process collaboration of "parameter optimization - cost assessment - constraint optimization" is formed, rather than a simple assembly of algorithms, ensuring that the scheduling scheme takes into account economy, accuracy and feasibility.

4. Performance Evaluation of Power System Economic Dispatch Model based on RCBA

4.1 Experimental Environment

In order to verify the superiority of the PSO-BPNN hybrid algorithm The study compares it with three algorithms: Differential Evolution Algorithm (DE), Firefly Algorithm (FA), and Whale Optimization Algorithm (WOA). All three are mainstream meta-heuristic algorithms in the field of economic dispatching of power systems, with strong global search capabilities. They respectively represent different types of optimization logics such as differential variation, luminance attraction, and encirculation prehunt. They are often used as performance comparison benchmarks in this field, and have strong parameter adjustability, which is convenient to keep core parameters such as population size and iteration times consistent with PSO-BPNN. Ensure the fairness of the experiment. To enhance the credibility of the results, study conducted 10 - fold cross-validation experiments for the two core datasets,

ISO-NE and ERCOT. The procedure involved randomly dividing each dataset into training and testing sets at a 7:3 ratio, repeating the division and model training/testing process 10 times, and then calculating the stability parameters of key metrics. Among them, the ISO-NE dataset covers load, ancillary service prices and renewable energy power generation data within five years. The corresponding system contains 100 units (30 coal-fired units, 20 gas-fired units and 50 new energy units), with a load range of 5,000 – 10,000MW. The ERCOT grid integrated dataset contains detailed information on node marginal electricity prices, generator output, and load forecasting curves. The corresponding system includes 150 units (40 coal-fired units, 30 gas-fired units, and 80 new energy units), with a load range of 8,000 to 12,000MW. The new energy output data are all sampled with a 10 -minute accuracy. The experiment covers two typical scheduling scenarios, namely the regular load scenario (with a daily fluctuation of $\pm 5\%$ in load) and the extreme load scenario (with a sudden increase of 20% in load).

4.2 Description of Experimental Reproducibility

- (1) Dataset: Both the ISO-NE and ERCOT datasets are public datasets.
- (2) Hardware requirements: Ordinary servers (CPUi7+GPU 1660 or above) can reproduce the results.

Practical application feasibility:

- (1) Computing resource requirements: A single server can support real-time scheduling of systems with less than 200 nodes, meeting the dispatching needs of regional power grids.
- (2) Scheduling time constraint: The optimization time required for day-ahead scheduling is ≤ 1 hour, and the maximum optimization time of the research model is 8.5 seconds, which fully meets the requirements. Real-time scheduling needs to be further lightweight and can be achieved through FPGA acceleration in the future.

4.3 Improved PSO-BPNN Fusion Algorithm Effect Verification

The study evaluated the fitness values of the four algorithms-PSO-BPNN, DE, FA, and WOA-on the two datasets. The fitness value directly corresponds to the forecast error of power generation costs. A smaller value indicates more accurate cost prediction, which can reduce the estimation deviation in dispatching decisions. The results are shown in Figure 7.

As shown in Figure 7(a), when training on the ISO-NE dataset, the fitness value of PSO-BPNN decreased significantly from 0 to 100 iterations. After 150 iterations, it gradually stabilized, and the fitness value reached 1000. The fitness value of WOA exhibited a downward trend during the first 120 iterations, and then stabilized at 10016 after 120 iterations. The decline curve of FA’s fitness value was similar to that of WOA, but its convergence speed was

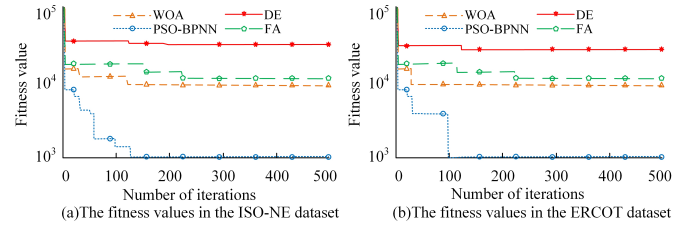


Figure 7. Comparison of Fitness Value Test Results

slightly slower than that of the WOA algorithm. After 220 iterations, the fitness value stabilized at 15026. Compared with the three algorithms mentioned above, the fitness value of DE decreased the least with the increase in iterations, stabilizing at 60057. As shown in Figure 7(b), when training on the ERCOT dataset, the fitness value of PSO-BPNN stabilized at 1000 after 98 iterations. The fitness value of the WOA algorithm stabilized at 10134 after 35 iterations, showing good convergence. The decreasing curve of FA’s fitness value did not show significant changes, and the fitness value remained stable at 15045 after 215 iterations. The fitness value of DE stabilized at 58003 after 119 iterations. The fitness value serves as a metric to evaluate the algorithm’s performance. A lower fitness value indicates higher prediction accuracy and better overall performance. In summary, PSO-BPNN demonstrated higher prediction accuracy and stronger convergence, which was significantly better than the comparison algorithms. To further prove the stability of the proposed algorithm, the Root Mean Square Error (RMSE) of the power generation cost for the four algorithms was compared and tested experimentally. The Root Mean Square Error (RMSE) measures the stability of cost forecasting. A more concentrated error distribution indicates lower volatility in scheduling plans, thereby preventing wind or solar curtailment and power supply shortages caused by forecasting fluctuations, and ensuring the ‘supply-demand balance’ objective. The test results are shown in Figure 8.

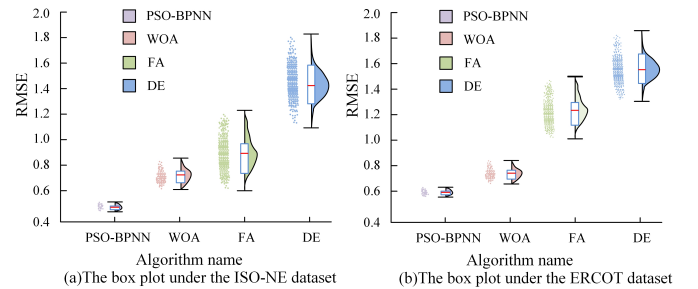


Figure 8. RMSE Comparison Results of Power Generation Cost

In Figure 8, the box plot of the ISO-NE dataset shows that the median RMSE of PSO-BPNN was 0.55 . At this point, the prediction error of PSO-BPNN was significantly lower than that of DE, at 1.42 , and the error reduction rate reached 60%. In the box plot of the ERCOT dataset, the median RMSE of PSO-BPNN was 0.63 , which was also lower than that of FA and DE . In addition, the box height

of PSO-BPNN was the narrowest in both datasets. Its interquartile range was only 0.12 in the ISO-NE dataset, and its telescopic length was short with no obvious outliers, indicating that its error distribution was more concentrated, and its stability and robustness were better. To further verify the learning and convergence of PSO-BPNN, the study continued to compare the F1 score of the four algorithms. The comparison results are shown in Figure 9.

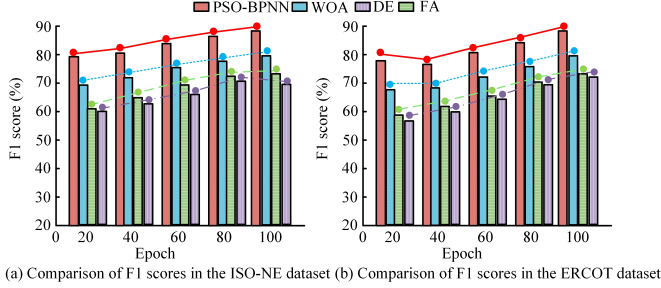


Figure 9. F1 Score Comparison Results of Four Algorithms

As shown in Figure 9(a), when the training rounds were 20 in the ISO-NE dataset, the F1 score of PSO-BPNN was about 78.9%, while that of WOA was about 67.5%. As the training rounds increased, PSO-BPNN always kept the lead. When the training rounds reached 100, the F1 score of PSO-BPNN reached 88.3%, while that of WOA was 79.2%. In each round, the F1 score of PSO-BPNN was about 10 percentage points higher than that of WOA, which fully reflected its better balance between precision and recall during model training. As shown in Figure 9(b), in the ERCOT dataset, PSO-BPNN showed higher F1 scores in each training stage and had better classification performance than the other algorithms.

4.4 Performance Evaluation Analysis of Fusion Model Based on PSO-BPNN and RCBA

After verifying the performance of the PSO-BPNN fusion algorithm, in order to further evaluate the performance of the PSO-BP-RCBA power system economic dispatch model, the study tested and compared it with the model based on the Multi-Objective Artificial Bee Colony algorithm (MO-ABC), the Multiverse Optimizer (MVO), and the Linear Programming and Genetic Algorithm (LP-GA). The experiment used PyTorch as the core deep learning framework, and the development environment used Anaconda 3. The hardware configuration consisted of an Intel Xeon Gold 6230R CPU, equipped with an NVIDIA GeForce RTX 3080 GPU, and the experimental data set still utilized the ISO-NE and ERCOT power grid comprehensive data sets. The study compared the power generation cost convergence curves of the four models in the same iteration cycle, and the results are given in Figure 10.

Figure 10. Comparison results of power generation cost convergence curves As shown in Figure 10, in the ISO-NE and ERCOT data sets, the power generation cost curves of the PSO-BP-RCBA model dropped rapidly in the early iterations, approaching the low-cost zone faster than the

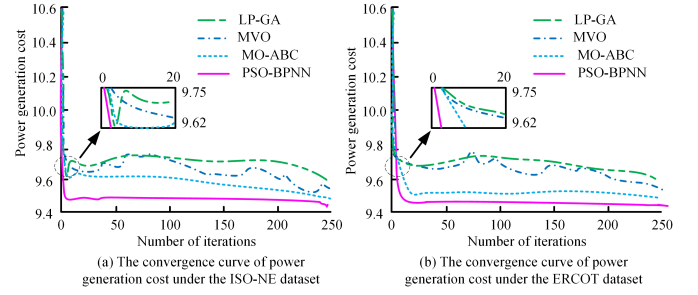


Figure 10. Comparison Results of Power Generation Cost Convergence Curves

LP-GA, MVO, and MO-ABC models. Finally, after 250 iterations, the power generation cost of the model stabilized at a minimum of 9.48. In contrast, the power generation costs of other models were higher than those of the research model. Furthermore, compared with the test results of Agushaka J O and other scholars on the convergence and accuracy of the BA algorithm model under the same test scale, the convergence speed of the research model has also been significantly improved [21]. This difference stems from the three-level closed-loop collaborative mechanism of the research model, which is "PSO parameter optimization -BPNN cost fitting -RCBA constraint optimization". It has overcome the limitations of single heuristic optimization, such as the imbalance between exploration and development and insufficient adaptation to high-dimensional scenarios. In summary, PSO-BP-RCBA exhibited a faster convergence speed and lower power generation cost, and its performance in optimizing power generation cost was superior to that of the comparison models, highlighting its advantages in the economic dispatch of power systems. To further verify the prediction accuracy of the PSO-BP-RCBA model, the study also compared the fit of the four models, with the comparison results presented in Figure 11.

As shown in Figure 11(a), the predicted points of PSO-BP-RCBA were closely around the straight line. When the actual value was 0.5, the expected value was 0.48, and when the actual value was -0.8, the expected value was -0.78. The Coefficient of Determination (R^2) was 0.98, with an average deviation of 0.02, indicating a high level of consistency between the predicted and actual values. As shown in the other three figures, the coefficient of determination R^2 of MO-ABC was 0.7, the R^2 of MVO was 0.7, and the R^2 of LP-GA was 0.6. Their predicted points were obviously scattered, with average deviations of 0.2, 0.2, and 0.3, respectively. In summary, the expected points of PSO-BP-RCBA were the most concentrated, and the fitting accuracy was the best, indicating significant superiority in the prediction task, which more accurately reflects the actual situation. To evaluate the real-time performance of the models in practical engineering applications, the study compared the time growth trends of single-scheduling optimization across four models under varying node scales, as shown in Figure 12.

As can be seen from Figure 12, the single scheduling op-

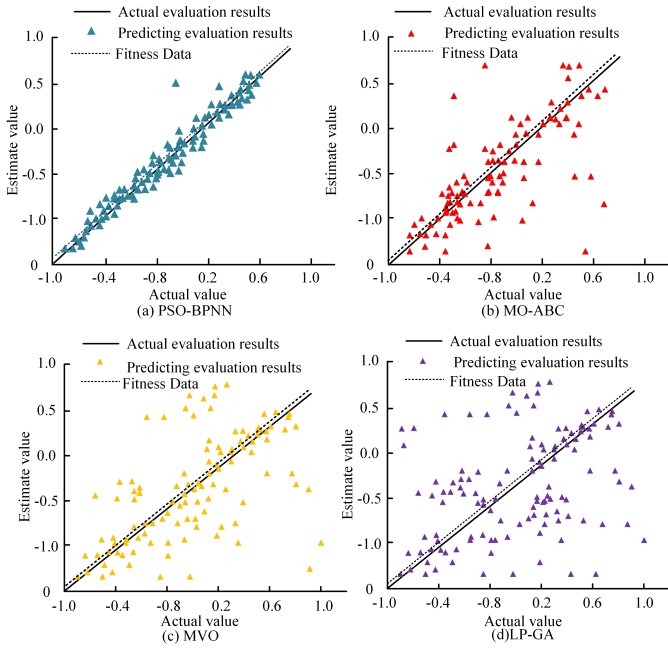


Figure 11. Comparison of the Prediction Accuracy Experimental Results

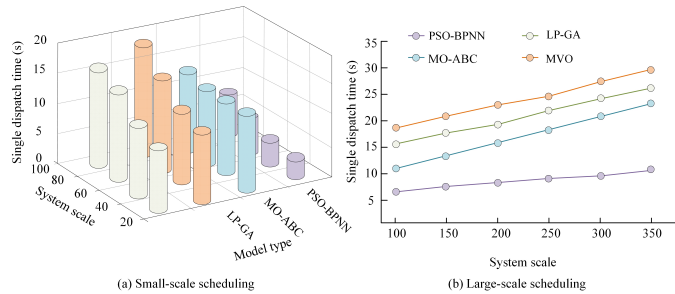


Figure 12. Comparison of the Time to Complete a Single Scheduling Optimization

timization time of the four models all increases with the increase of the training scale. However, the overall scheduling optimization time of PSO-BP-RCBA is shorter. In the context of small-scale nodes as shown in Figure 12(a), when there are 20 nodes, the scheduling of PSO-BP-RCBA only takes 3.2 seconds (scheduling scale: 50 units, load 5000 MW, new energy penetration rate 20%). In the context of large-scale nodes as shown in Figure 12(b), when the training scale reaches 350, its scheduling time only slightly increases to 11.2 seconds. However, the increase in the single scheduling optimization time of the comparison models MO-ABC, MVO and LP-GA is much higher than that of the research model. Furthermore, in order to achieve low-latency resource scheduling, the Yin C team proposed a new genetic ant colony optimization algorithm model. Experimental results show that compared with this optimization model, the single scheduling optimization time of the research model is also shorter [22]. The shorter the time for a single scheduling optimization, the stronger the real-time performance and scalability of the model. Therefore, the experimental results show that the PSO-BP-RCBA model

has a higher computational efficiency in processing data.

5. Conclusion

To address the inefficiencies in handling nonlinear constraints and the weak adaptability to renewable energy in power system economic dispatch, the study designed a PSO-BP-RCBA economic dispatch model. This model uses BPNN to fit complex cost functions, combines PSO for global search optimization of variable decisions, and applies RCBA to suppress interference paths. The experimental results show that the PSO-BP-RCBA model achieves a performance breakthrough through the synergy of core mechanisms. The global search ability of PSO solves the local optimum problem of the initial parameters of BPNN, enabling it to converge rapidly and have excellent fitting accuracy (median RMSE 0.55, coefficient of determination $R^2 = 0.98$). RCBA integrates the local optimization characteristics of bats and the global exploration features of random black holes. Supported by the precise cost assessment of BPNN, it efficiently searches for the optimal scheme that satisfies multiple constraints (the power generation cost is stable at 9.48, with an average deviation of 0.02), and its scheduling efficiency is significantly better than that of the comparison model (the fastest single optimization is 3.2 seconds). The core innovation of the model is reflected in three aspects: (1) It builds a three-level fusion closed loop of "PSO parameter optimization -BPNN cost fitting -RCBA constraint optimization", specifically addressing the shortcomings of a single algorithm; (2) Introduce the random black hole model to improve BA, balancing global exploration and local optimization; (3) Replace the traditional analytical cost function with data-driven BPNN to enhance adaptability in high-dimensional scenarios. However, the current research has certain limitations. For instance, the existing size of the model is difficult to adapt to embedded terminals, there is still room for optimization in real-time performance in large-scale scenarios, the engineering deployment verification has not yet been completed, and the decision-making process lacks interpretability. Future work will focus on the following implementation paths:

- (1) Model lightweighting: By using neural network pruning (structured pruning of hidden layer neurons) and quantization techniques, the model volume will be compressed to adapt to embedded scheduling terminals;
- (2) Hardware acceleration: Parallel computing of the RCBA core module is implemented based on FPGA to compress the single scheduling time and meet the real-time scheduling requirements.
- (3) System integration: Develop API interfaces with existing EMS, complete the engineering deployment of the pilot power grid, and verify the actual operation effect;
- (4) Enhance model interpretability: Introduce an attention mechanism to label the key input features of BPNN, and extract scheduling rules from the opti-

Table 1
Comparison of Core Performance with the Baseline Algorithm

Algorithm Name	Average Power Generation Cost (10,000 yuan/hour)	Convergence Iterations	Constraint Satisfaction Rate	Single Scheduling Time (s)
PSO-BP-RCBA	9.48	250	100%	3.2
Standard Bat Algorithm (BA)	12.86	320	89%	5.7
Swarm Optimization (PSO)	11.35	280	91%	4.8
Genetic Algorithm (GA)	11.53	350	92%	6.1

mization results of RCBA through the decision tree algorithm to improve the acceptance of the actual power system. To further validate the model's superiority over traditional basic algorithms, we supplement core performance metrics as shown in Table 1.

Note: All data are based on 100 units and a 40% renewable energy penetration scenario, with averages calculated from 10 repeated experiments. The constraint satisfaction rate refers to the percentage of experiments that simultaneously meet power balance, unit output limits, and ramp rate constraints.

Fundings

The research is supported by The Soft Science Special Project of Gansu Basic Research Plan (Grant No. 24JRZA063, China).

Conflicts of interest

All authors declare that they have no conflicts of interest.

References

- [1] A. Raihan, "Green energy and technological innovation toward a low-carbon economy in bangladesh," *Green and Low-Carbon Economy*, vol. 3, no. 2, pp. 171–181, 2025.
- [2] J. Li, Y. Peng, Z. Yang, and J. Pan, "Virtual power plant economic dispatch model based on parallel molecular differential evolution algorithm," *International Journal of Power and Energy Systems*, vol. 45, no. 2, pp. 64–77, 2025.
- [3] D. Wang, N. Gao, D. Liu, J. Li, and F. L. Lewis, "Recent progress in reinforcement learning and adaptive dynamic programming for advanced control applications," *IEEE/CAA Journal of Automatica Sinica*, vol. 11, no. 1, pp. 18–36, 2023.
- [4] J. Lin and Q. Sun, "A low carbon economic optimal dispatching model for comprehensive energy system based on improved whale algorithm," *International Journal of Power and Energy Systems*, vol. 44, pp. 1–12, 2024.
- [5] R. Fei, Y. Guo, J. Li, B. Hu, and L. Yang, "An improved bpnn method based on probability density for indoor location," *IEEE Transactions on Information and Systems*, vol. 106, no. 5, pp. 773–785, 2023.
- [6] S. Sobhanayak, "Mohba: Multi-objective workflow scheduling in cloud computing using hybrid bat algorithm," *Computing*, vol. 105, no. 10, pp. 2119–2142, 2023.
- [7] M. H. Seifipour and H. Abdi, "Solving the economic dispatch problem by using wild horse optimizer algorithm," *Research and Technology in the Electrical Industry*, vol. 3, no. 2, pp. 361–372, 2024.
- [8] S. P. M. Lialestani, D. Parcerisa, M. Himi, and A. A. Shahri, "A novel modified bat algorithm to improve the spatial geothermal mapping using discrete geodata in catalonia-spain," *Modeling Earth Systems and Environment*, vol. 10, no. 3, pp. 4415–4428, 2024.
- [9] Y. K. Saheed, T. O. Kehinde, M. A. Raji, and U. A. Baba, "Feature selection in intrusion detection systems: A new hybrid fusion of bat algorithm and residue number system," *Journal of Information and Telecommunication*, vol. 8, no. 2, pp. 189–207, 2024.
- [10] S. Heddami, S. Kim, A. D. Mehr, M. Zounemat-Kermani, M. Ptak, A. Elbeltagi, and Y. Tikhamarine, "Bat algorithm optimised extreme learning machine (bat-elm): A novel approach for daily river water temperature modelling," *The Geographical Journal*, vol. 189, no. 1, pp. 78–89, 2023.
- [11] Q. Luo, F. Garcia-Menendez, H. Yang, R. Deshmukh, G. He, J. Lin, and J. X. Johnson, "The health and climate benefits of economic dispatch in china's power system," *Environmental Science & Technology*, vol. 57, no. 7, pp. 2898–2906, 2023.
- [12] Q. Liu, G. Xiong, X. Fu, A. W. Mohamed, J. Zhang, M. A. Al-Betar, and S. Xu, "Hybridizing gaining-sharing knowledge and differential evolution for large-scale power system economic dispatch problems," *Journal of Computational Design and Engineering*, vol. 10, no. 2, pp. 615–631, 2023.
- [13] F. She, F. Li, H. Cui, J. Wang, Q. Zhang, and R. Bo, "Virtual inertia scheduling (vis) for real-time economic dispatch of ibr-penetrated power systems," *IEEE Transactions on Sustainable Energy*, vol. 15, no. 2, pp. 938–951, 2023.
- [14] S. Lei, S. Bu, Q. Wang, Q. Chen, L. Yang, and Y. Chi, "Look-ahead rolling economic dispatch approach for wind-thermal-bundled power system considering dynamic ramping and flexible load transfer strategy," *IEEE Transactions on Power Systems*, vol. 39, no. 1, pp. 186–202, 2023.
- [15] B. Pan, B. Hu, C. Shao, L. Xu, K. Xie, Y. Wang, and A. Anvari-Moghaddam, "Reliability-constrained economic dispatch with analytical formulation of operational risk evaluation," *IEEE Transactions on Power Systems*, vol. 39, no. 2, pp. 4422–4436, 2023.
- [16] K. A. Khatri, K. B. Shah, J. Logeshwaran, and A. Shrestha, "Genetic algorithm based techno-economic optimization of an isolated hybrid energy system," *CRF*, vol. 8, no. 4, pp. 1447–1450, 2023.
- [17] M. Mesquita-Cunha, J. R. Figueira, and A. P. Barbosa-Póvoa, "New ϵ -constraint methods for multi-objective integer linear programming: A pareto front representation approach," *European Journal of Operational Research*, vol. 306, no. 1, pp. 286–307, 2023.
- [18] L. Yang and N. Engelhardt, "The complexity of learning (pseudo) random dynamics of black holes and other chaotic systems," *Journal of High Energy Physics*, vol. 2025, no. 3, pp. 1–65, 2025.
- [19] R. K. Tipu, V. Batra, Suman, K. S. Pandya, and V. R. Panchal, "Predicting compressive strength of concrete with iron waste: A bpnn approach," *Asian Journal of Civil Engineering*, vol. 25, no. 7, pp. 5571–5579, 2024.
- [20] T. Sabharwal and R. Gupta, "Human face identification after plastic surgery using surf, multi-knn and bpnn techniques," *Complex & Intelligent Systems*, vol. 10, no. 3, pp. 4457–4472, 2024.

- [21] J. O. Agushaka, A. E. Ezugwu, L. Abualigah, S. K. Alharbi, and H. A. E. W. Khalifa, "Efficient initialization methods for population-based metaheuristic algorithms: A comparative study," *Archives of Computational Methods in Engineering*, vol. 30, no. 3, pp. 1727–1787, 2023.
- [22] C. Yin, Q. Fang, H. Li, Y. Peng, X. Xu, and D. Tang, "An optimized resource scheduling algorithm based on ga and aco algorithm in fog computing," *The Journal of Supercomputing*, vol. 80, no. 3, pp. 4248–4285, 2024.

Biographies



Tingxi Wang received his Ph.D. in Theoretical Economics from Beijing Normal University. He is currently an Associate Professor, Master's Supervisor, and Head of the Economics Department at the School of Economics, Northwest Normal University. His research interests include the digital economy and the intelligent computing industry.